Bulletin of Geophysics and Oceanography Vol. XX, n. X, pp. XXX-XXX; Xxxxx 20xx
DOI 10.4430/bgo00455

Empirical spectral amplification functions using strong ground motion data and the mixed effect analysis method: application in Algeria

F. Gherboudj, T. Ouzandja and R. Bensalem

National Center of Applied Research of Earthquake Engineering, CGS, Algiers, Algeria

(Received: 20 July 2023; accepted: 14 February 2024; published online: 19 April 2024)

ABSTRACT This paper aims to calculate empirical spectral amplification functions for multiple locations in the north central region of Algeria by utilising strong ground motion records of earthquakes occurring in this region ($M \geq 4$). The analysis consists in performing a residual analysis of the observed ground motions in relation to the local ground motion prediction equation (GMPE). This task is achieved through the application of the mixed effect analysis method to divide the total residuals into between-event residuals (source effect) and within-event residuals (site effect). For instance, the reference site, situated on a rocky formation near the Keddara dam, shows clear deamplification for periods longer than 0.2 s with respect to the GMPE with V_{s30} = 800 m/s. Furthermore, other sites located in urban areas within the Mitidja basin, such as Boufarik, display distinct amplification in the long-period range, which underscores the importance of considering basin effects within the Mitidja basin. Ultimately, based on the derived amplification functions, the local GMPE is adjusted by incorporating the site term. This modification aims to improve the accuracy of surface ground motion prediction in site-specific probabilistic seismic hazard analysis near the selected sites.

Key words: mixed effect analysis, empirical amplification function, strong motion, adjusted GMPE, Mitidja basin effect.

1. Introduction

A probabilistic seismic hazard analysis (PSHA) integrates seismic source characteristics and the ground motion prediction equation (GMPE) to estimate the seismic intensities for a specific site. This is done on the basis of the magnitude, location, and local geology of the future earthquakes. Site effects, primarily represented by shear wave velocity in the upper 30 m of the soil profile (V_{s30}), following the ergodic assumption (Anderson and Brune, 1999), are implicitly included within the GMPE. However, in site-specific PSHA studies, there is a tendency to mitigate the ergodicity assumption. Consequently, by considering the site-specific effect through an amplification function, efforts are made to reduce the aleatory variability (sigma) associated with the site effects by adjusting the predicted median ground motion. This approach is known as a partially non-ergodic site-specific PSHA (Atkinson, 2006; Rodriguez *et al*., 2014; Stewart *et al*., 2017).

Despite its limitations in soil modelling (1D versus 2D/3D), the 1D numerical analysis, using the linear equivalent method, is commonly employed in site-specific PSHA to estimate the amplification function. Additionally, empirical approaches based on strong motion data can

enhance the characterisation of the site effects by using either the reference or non-reference site method (Stewart *et al*., 2014). Amplification functions can, in fact, be estimated by comparing the spectral ratio between observed ground motions from two nearby sites: one with soft soil and the other with rock soils [reference site approach (Borcherdt and Gibbs, 1970; Borcherdt and Glassmoyer, 1994)], or by comparing the spectral ratio between observed ground motions and the mean predicted ground motion [non-reference site approach (Stewart *et al*., 2003)].

For instance, Si *et al*. (2010) used the latter approach to remove the site effects from strong motion data while studying the hanging wall effect of the 1994 Northridge earthquake. Ibrahim *et al*. (2014) also used strong motion records to derive empirical spectral amplification functions for 75 sites in the Iwate-Miyagi and Niigata regions. The abundance of data from a dense array in Japan made it easier to calculate amplification functions by simply adding and averaging the spectral ratios. Additionally, the non-reference site approach is used in determining site amplification during the development of GMPEs (Atkinson, 2015).

In this study, we propose estimating the empirical amplification functions of several sites within the Algerian strong motion network by means of available strong motion data from the central part of Algeria. To address the limited amount of data, the mixed effect analysis (MEA) was employed to perform a residual analysis of the observed ground motions relative to the local GMPE (Laouami *et al*., 2018). Initially, the analysis was conducted for the reference site, Keddara Boumerdes (KDRA), situated near the Keddara dam in the Boumerdes region. This site is characterised by rock soil with a metamorphic basement composed of mica schist and gneiss from the Palaeozoic era. The strong motion records of the 2003 Boumerdes earthquake, recorded by the KDRA station, have been extensively used in seismic risk analysis as input motion for soil profiles or structures (e.g. JICA, 2006). For this reason, the accurate determination of the amplification function of this site is of paramount importance.

Additionally, despite the limited data, investigations are being conducted at other sites, as well as at specific stations located in urban areas in the city of Algiers and within the Mitidja basin. The goal of this study is to estimate the amplification function across a wide range of periods, so as to enhance the understanding of the strong motion recorded and the basin effect in this sensitive region given its significant and rapid urban and economic development. Lastly, based on the derived amplification functions, the local GMPE is adjusted by incorporating the site term. The observed motions are, then, compared to the predicted motions using both the original GMPE and adjusted GMPE.

2. Strong motion data

Strong motion data used in this study are obtained through the strong motion network managed by the Research Center of Earthquake Engineering (www.cgs-dz.org), which covers the entire northern part of Algeria. Time history accelerations were recorded by ETNA digital accelerographs with a sampling frequency of 200 Hz. Following instrument correction and baseline correction of acceleration, a 25 Hz low-pass filter type Ormsby was applied together with a 0.2 Hz high-pass filter.

Only events recorded by at least three stations (including the site subject taken in consideration herein), among all earthquakes with a magnitude of $M \geq 4.0$ and with a hypocentral distance less than 200 km, are considered in this study. Table 1 shows 17 selected earthquakes with records provided by a total of 43 stations (Fig. 1), including stations where site effect analyses were carried out.

Table 1 - Events considered in this study (M_w > 4.0).

Date	Time	M_w	Depth (km)	Location
4 Sept. 1996	-	5.5	10	36.96 N - 2.91 E
21 May 2003	18:44:21	6.8	12	36.98 N - 3.36 E
27 May 2003	17:11:29	5.7	8	36.94 N - 3.58 E
28 May 2003	06:58:41	5	10	36.88 N - 3.27 E
29 May 2003	02:15:02	4.9	10	36.82 N - 3.36 E
10 Jan. 2004	18:38:15	4.7	10	36.99 N - 3.37 E
1 Dec. 2004	18:42:49	4.5	10	36.85 N - 3.45 E
5 Dec. 2004	08:30:59	4.4	10	36.92 N - 3.38 E
22 July 2006	13:22:22	4.0	5	36.97 N - 2.96 E
1 Feb. 2008	07:33:40	4.6	10	36.83 N - 3.47 E
17 July 2013	-	5.2	10	36.52 N - 2.93 E
22 Feb. 2014	19:30:15	4.3	14	36.81 N - 3.66 E
1 Aug. 2014	04:11:16	5.5	10	36.86 N - 3.18 E
28 May 2016	00:53:17	5.4	10	36.46 N - 3.56 E
10 Feb. 2016	02:28:20	4.6	10	36.54 N - 3.08 E
16 May 2016	10:18:00	4.7	18	36.36 N - 3.45 E
2 Jan. 2018	-	4.7	10	36.43N - 2.54 E

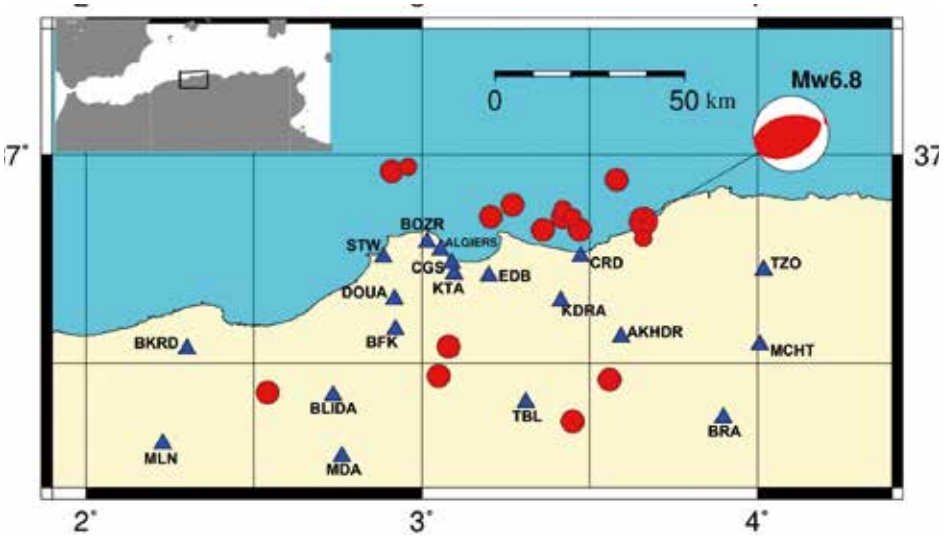

Fig. 1 - Sketch map illustrating events considered in this study (red circles; the size of each circle is proportional to its magnitude) recorded at stations indicated with the blue triangles.

The local GMPE of Laouami *et al*. (2018) is used in this study to calculate the total residuals of the recorded seismic ground motion relative to the GMPE. This equation was mainly developed on the basis of local strong motion (over 700 records).

The peak ground acceleration (*PGA*) and pseudo spectral acceleration (*PSA*) for each oscillator period, *T,* with respect to the moment magnitude, M_W, and hypocentral distance, R_{hypo}, are expressed as follows:

$$log_{10}PSA(T) = a(T)M_w + b(T)R - log_{10}R + c_{1,2,3}(T) + \sigma(T). \quad (1)$$

This GMPE includes the source term [$a(T)M_w$], the geometrical spreading (-$log_{10}R$), in other words 1/R, and the path anelastic attenuation term through the $b(T)$ coefficient. Site effect is considered through factors c_1, c_2, or c_3, which correspond to three soil classes: rock (S1: $V_{s30} \geq 800$ m/s), firm (S2: 400 m/s ≤ $V_{s30} < 800$ m/s), and alluvium (S3: $V_{s30} < 400$ m/s), respectively.

Fig. 2 shows an example of two events, the 2004 M 4.7 and the 2014 M 5.5, recorded at several stations. Fig. 3 shows the comparison between the observed values and those obtained using the GMPE.

a. 10 Jan. 2004 (M_w 4.7)

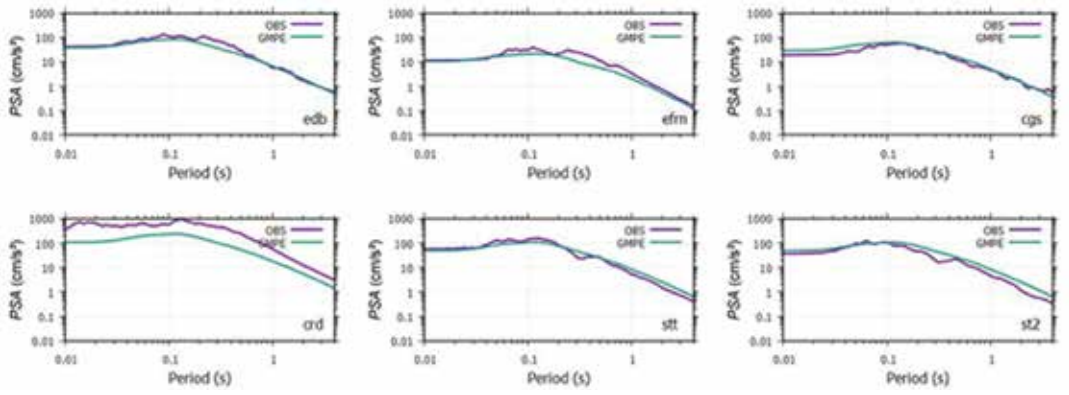

a

b. 1 Aug. 2014 (M_w 5.5)

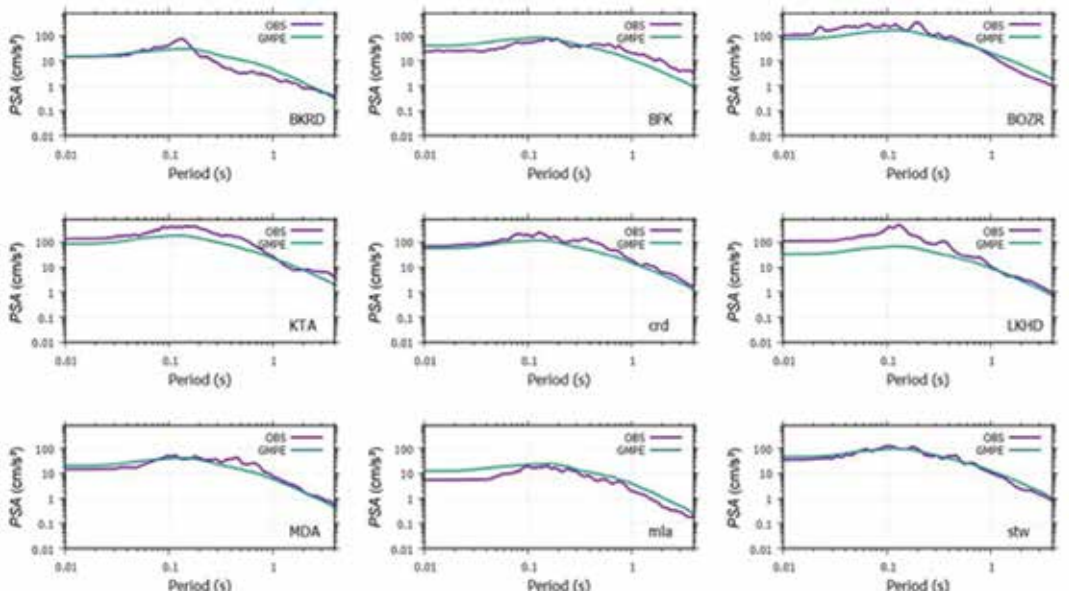

b

Fig. 2 - Example of 5%-damped acceleration response spectra for two events: M_w 4.7 on 10 January 2004 (a) and M_w 5.5 on 1 August 2008 (b) recorded at several stations and compared using the GMPE of Laouami *et al*. (2018).

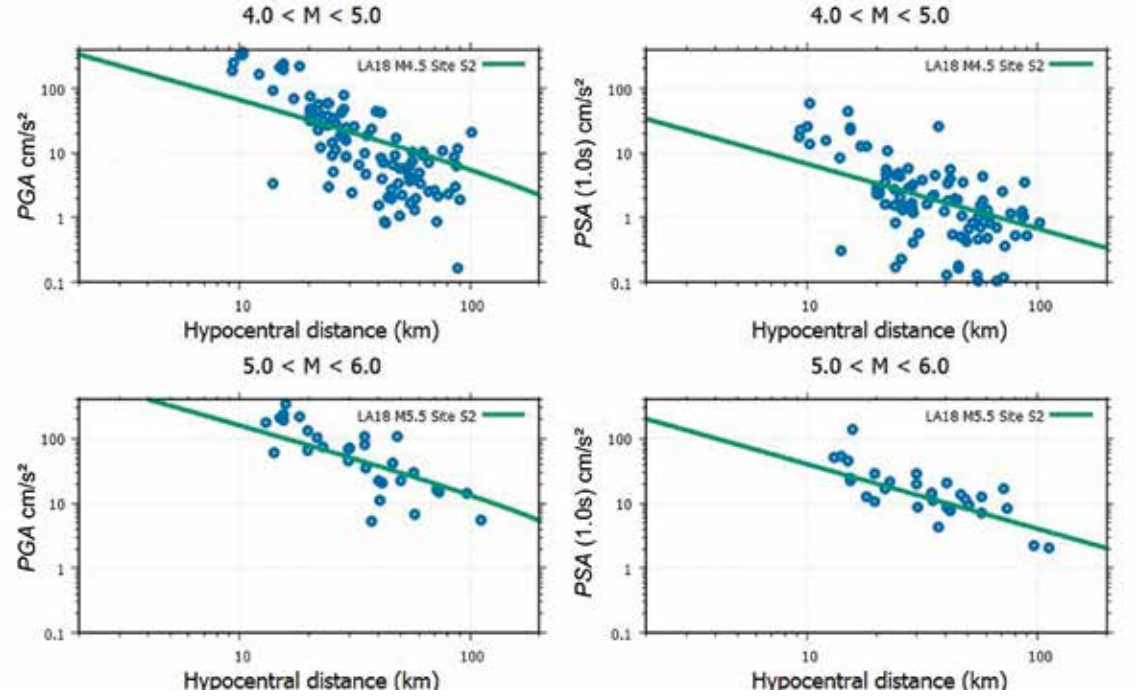

Fig. 3 - *PGA* (left panels) and *PSA* (1.0 s) (right panel) of the two data sets, at the top 4.0 < *M* < 5.0 and at the bottom 5.0 < *M* < 6.0. Green lines are computed using the GMPE of Laouami *et al*. (2018).

3. Site selection and classification

The selected sites (red triangles) analysed in the next section and shown in Fig. 4, belong to the national strong motion network. Additional measurements of ambient vibrations and horizontal-to-vertical spectral ratio (HVSR) are computed by calculating the spectra amplitude ratio of horizontal and vertical components of ambient vibratory noise. This method is widely used in site effect and microzonation studies, to obtain the fundamental ground resonance frequency (Bensalem *et al*., 2010, 2017; Hellel *et al*., 2010). The acquisition of ambient noise in a free field was carried out in the vicinity of the accelerometer stations. According to the recommendations of SESAME (2004), 12 recording points of 15 minutes each were performed using a CityShark station coupled to a Lennartz 5-second 3-component seismometer, with a 200-Hz sample rate. Analyses of the HVSR data were processed using Geopsy software (Wathelet *et al*., 2020), where only 50 stable windows were used to ensure a good estimate of the low frequency bound. Fig. 5 shows an example of the HVSR obtained for the two sites: BFK (Boufarik) and TBL (Tablat) stations. In the next section, the mean microtremor HVSR of the nine selected sites is compared with the empirical amplification functions.

Shear wave velocity profiles are available for four stations: EDB, CRD, CGS and KTA (Guillier *et al*., 2005; JICA, 2006). While Meslem *et al.* (2010) conducted an evaluation of the site effect with the use of the HVSR of earthquake motions and the 1D numerical analysis, Laouami and Slimani (2013) conducted the site effect analysis for the three sites (EDB, CGS and CRD) using the microtremor HVSR method and comparing the results obtained with the HVSR of weak and strong earthquakes.

Moreover, Laouami *et al*. (2018) conducted an earthquake HVSR analysis to estimate the soil period and define the site classification using the method of Zhao *et al*. (2006). Table 2 summarises all the information for each selected site, namely the fundamental period, site classification, and average V_{s30} velocity (if available).

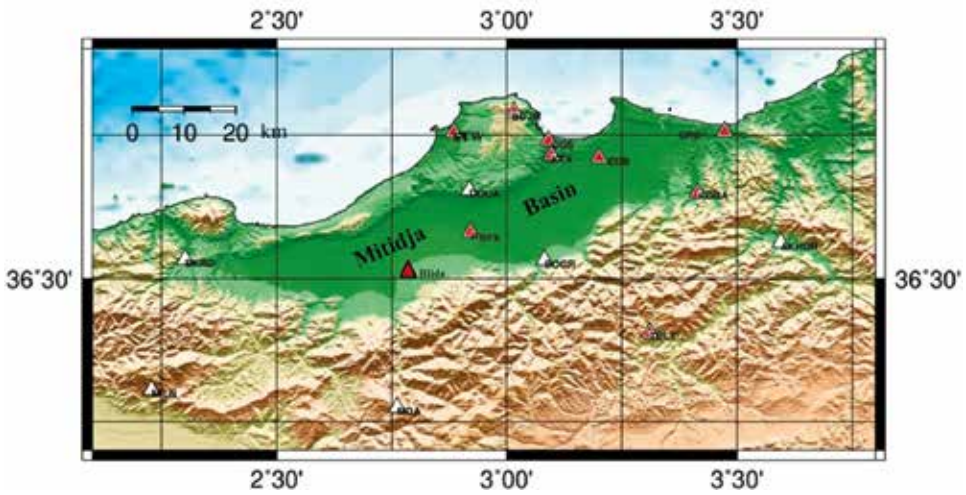

Fig. 4 - MNT map showing the selected sites (red triangles) and their location with respect to the Mitidja basin.

Table 2 - Site characteristics of the selected sites investigated in this study.

Site name (location)	Latitude - Longitude	Site period T_0	V_{s30}	Site classification
KDRA (Keddara Boumerdes)	36.65 N - 3.41E	0.1	784	S1
EDB (Dar El Beida)	36.71 N - 3.55 E	0.27	500	S2
CRD (Boumerdes)	36.75 N - 3.47 E	0.27	480	S2
BFK (Boufarik)	36.58 N - 2.92 E	1.13	–	S3
STW (Stawali)	36.75 N - 2.88 E	0.13	–	S1
BOZR (Bouzarea)	36.78 N - 3.02 E	–	890	S1
CGS (H dey)	36.74 N - 3.09 E	–	500	S2
KTA (Kouba)	36.71 N - 3.24 E	–	483	S2
Blida (Blida)	36.48 N - 2.81 E	0.7	–	S3
TBL (Tablat)	36.40 N - 3.31 E	0.16	–	S1

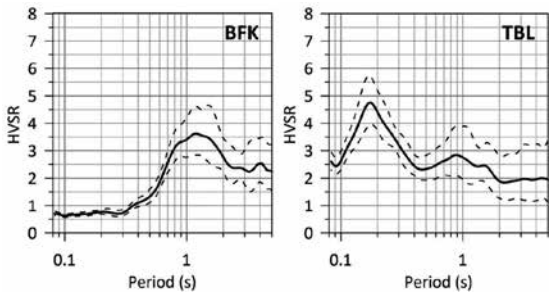

Fig. 5 - Example of the microtremor HVSR analysis conducted in this study for two selected sites: Tablat (TBL) and Boufarik (BFK).

4. Residual partition using mixed effect analysis

The difference between the predicted motion and the observed motion, called residual, is related to source effect, path effect, and site effect. A residual analysis is conducted in this section to extract the site effect terms for a set of selected stations.

Total residual R_{ij} of event *i* on target site *j* is expressed as follows:

$$R_{ij} = ln\,(z_{ij}{}^{obs}) - (\mu_{lnz})_{ij} \tag{2}$$

where:
μ_{lnz} is provided by the GMPE in terms of magnitude *M*, distance *R*, and site classification using Eq. 1; $z_{ij}{}^{obs}$ is the recorded 5% surface response spectrum, which is the geometrical mean of the two response spectra components (N-S and E-W), as follows:

$$z_{ij}{}^{\mathrm{obs}} = \sqrt{PSA^{\mathrm{north}}(T) * PSA^{\mathrm{south}}(T)}\,. \tag{3}$$

The total residuals (R_{ij}) of *PGA* and *PSA* (1.0 s) versus the magnitude and hypocentral distance, using GMPE of Laouami *et al*. (2018), are shown in Fig. 6 for all records and stations used in this study.

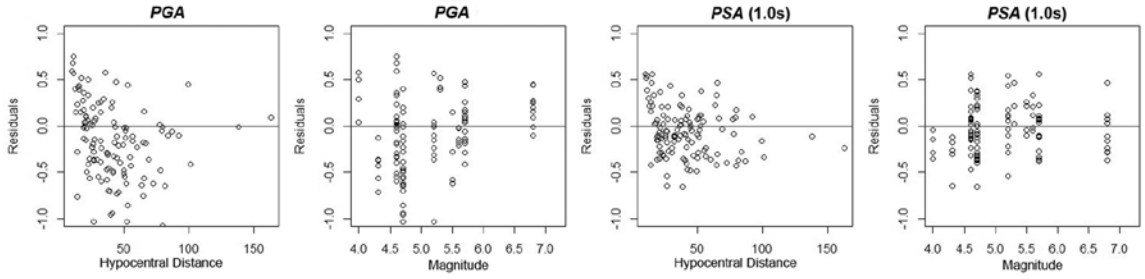

Fig. 6 - Total residuals (R_{ij}) for *PGA* and *PSA* (1.0 s) versus the magnitude and hypocentral distance (km).

R_{ij} contains effects relating to between-event term δE_i (source effect) and within-event term δW_{ij} (path and site effect) related to each event *i* and site *j* (Baltay *et al*., 2017; Sahakian *et al*., 2018). Two methods are proposed in the literature to conduct the partition of the total residual as described in the following.

4.1. Least-squares method (L2)

The regression using the least-squares method (L2) assumes that the distribution of the data (residuals) is normal with an unknown mean and standard deviation. The maximum likelihood estimator of the mean is the sample average, whereas the maximum likelihood estimator of the standard deviation is the sample's standard deviation divided by the square root of the number of data observations. More details on the approach applied in residual analyses in the context of

seismic motion data are provided in Appendix A in Stewart *et al*. (2017), in which the event and site terms are estimated as follows:

- The total residual can be partitioned into two components, the source term and the path and site term, as follows:

$$R_{ij} = \delta W_{ij} + \delta E_{i.} \tag{4}$$

- The mean event term, δE_i, is derived by simply averaging the total residuals of all N_i records of each earthquake *i* relative to the predicted motions by the GMPE (Stewart *et al*., 2017):

$$\delta E_i := \frac{1}{N_i} \sum_{j=1}^{N_i} R_{ij}. \tag{5}$$

After removing the event term from the total residual (Eq. 6), the site term component, η_s, can, then, be approximately determined by averaging the within-event residual (Eq. 7) from each record for the same site *j*:

$$\delta W_{ij} = R_{ij} - \delta E_i \tag{6}$$

$$\eta_{sj} = \frac{1}{N_j} \sum_{i=1}^{N} \delta W_{ij} \tag{7}$$

where N_j is the total number of events recorded on site *j*.

However, the application of the L2 method depends on the size of the available database (Stewart *et al*., 2017).

4.2. Mixed effect analysis (MEA)

This method, dealing with both fixed and random effects, seeks to capture repeated effects, such as source effects of an earthquake recorded by several stations or site effects from several records of different events on the same site (Abrahamson and Youngs, 1992; Stafford, 2014). The random effect is referred to as the between-event residual and is related to the source effect (δE_i). The remaining portion is called within-event residual and related to site and path effect δW_{ij}. The fixed effect is the overall model bias. Therefore, the linear mixed effect model is presented in this study as:

$$R_{ij} = c + \delta E_i + \delta W_{ij} \tag{8}$$

where δE_i and δW_{ij} are the random effect coefficients related to two grouping factors, earthquake and station, respectively, and *c* is the fixed effect, which represents the mean offset of the data relative to the selected GMPE.

Following Parker *et al*. (2020), two regression analyses are conducted to obtain the mixed effect model coefficients: the first MEA is carried out to derive fixed effect coefficient *c* and random event coefficients of δE_i and δW_{ij} using the lme4 package in R statistic (Bates *et al*.,

2015; R Core Team, 2019). In this step, the actual site effect for each station (43 stations) is considered on the basis of site classification as already considered by Laouami *et al*. (2018). The site characteristics of the nine selected sites are provided in the previous section (Table 2).

Fig. 7a shows the variation of the obtained coefficient of fixed effect *c* using three GMPEs: LA18 of Laouami *et al.* (2018), AK14 of Akkar *et al.* (2014), and BO14 of Boore *et al.* (2014). LA18 and AK14 were found to lead to minimal *c* values [less than 0.05 (log unit) in long periods]. Both equations are elaborated based on Mediterranean strong motion data. *c* values smaller than 0 are obtained in short periods using LA18 equations and positive values are obtained using equation AK14. It can, then, be concluded that this effect is far from being negligible for the law of Laouami *et al.* (2018), and that this offset must be removed from the total residual in order to maintain the hypothesis of zero mean random variables of the between-event term random and the within-event term random. Moreover, standard deviation of the random effects of δW_{ij} and δE_i, which decrease in long periods until they reach 0.15 for the two components, are shown in Fig. 7b.

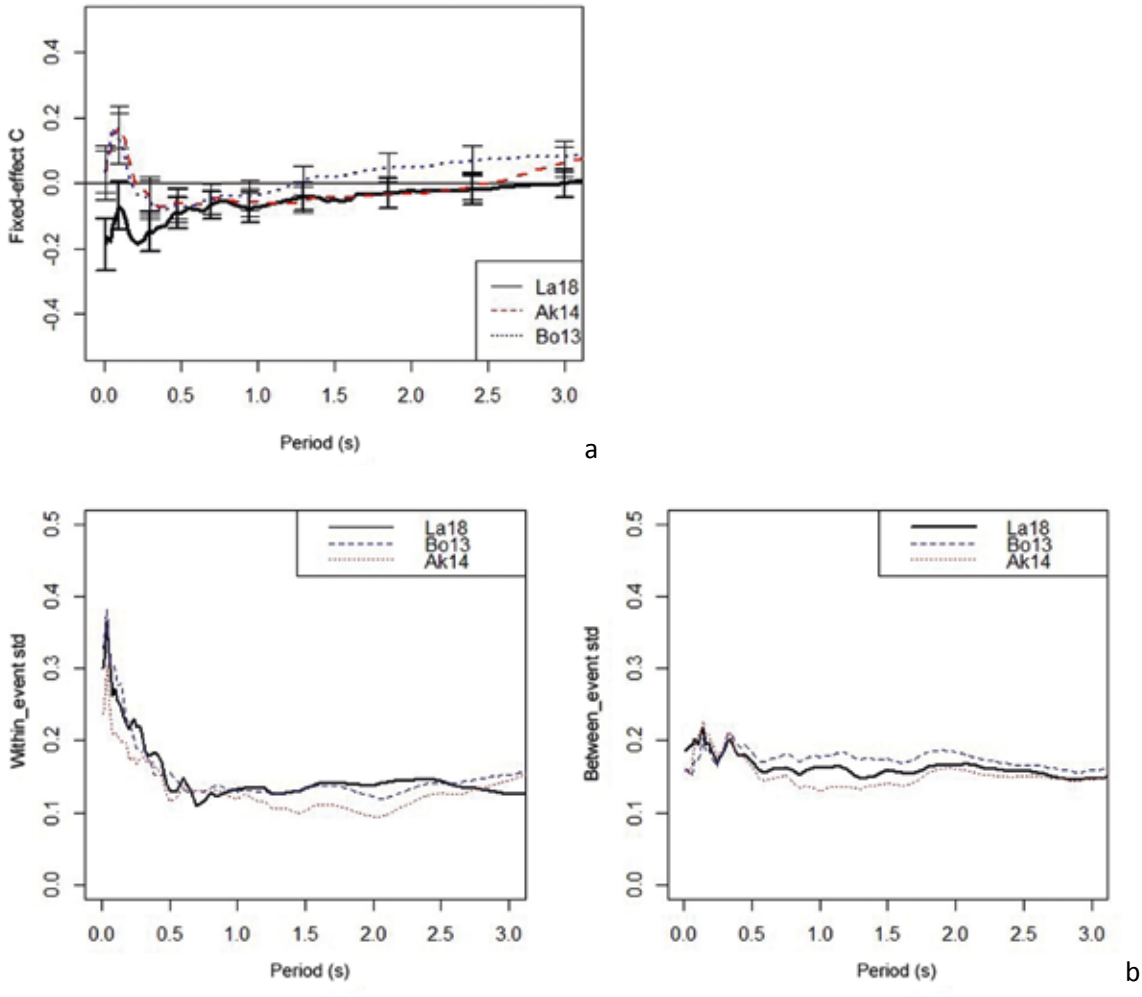

Fig. 7 - Fixed effect factor *c* (a) and standard deviation of random effect (b) (within-event and between-event terms) using three GMPEs.

Next, the total residuals are once again computed, with respect to the predicted motion on rock soil (V_{s30} = 800 m/s), as follows:

$$R_{ij} = \ln(z_{ij}) - \left(\mu_{lnz_{Vs30=800\frac{m}{s}}}\right)_{ij}. \quad (9)$$

The between-event term and fixed effect term already obtained in the first MEA are removed from the total residuals as follows:

$$\delta W_{ij} = R_{ij} - \delta \mathrm{E}_i - c. \quad (10)$$

Next, the second MEA is conducted to divide within-event residual δW_{ij} into site terms and remaining residuals epsilon ε_{ij} as follows:

$$\delta W_{ij} = \eta_{Sj} + \varepsilon_{ij}. \quad (11)$$

The remaining variability (ε_{ij}) corresponds to the event-to-event variability and path-to-path variability at station *j* (Stewart *et al*; 2017; Parker *et al*; 2020).

Ultimately, obtained site term η_{Sj} represents the empirical amplification function of the station considered in relation to the predicted ground motion at the bedrock (V_{s30} = 800 m/s).

5. Empirical amplification function results

The empirical amplification functions are presented in Figs. 8 and 9 and indicated with solid black lines. The within-event terms were obtained for each recorded earthquake used in this analysis. Additionally, the spectral ratios of the microtremor horizontal-to-vertical curves are displayed. In most cases, there is a reasonable agreement between the HVSR curves and the amplification functions in terms of fundamental frequencies and curve shape. The results for each site are given in the following discussion.

Initially, the site KDRA, located near the Keddara dam in Boumerdes, was selected as the reference site due to its location on a rocky formation composed of gneiss with a thin surface layer of soil. At KDRA, HVSR deamplification, with respect to the GMPE (V_{s30} = 800 m/s) curve, exhibits a flat shape with a prominent peak around 15 Hz, indicating a rock soil classification based on its fundamental period (Zhao *et al*., 2006). For this site, a total of ten events with magnitudes greater than 4.0 are utilised in this study, employing both the MEA method and the L2 method. The empirical amplification functions derived using these two methods are shown in Fig. 8. The values of the site factors obtained through the MEA method are lower than those obtained using the L2 method. However, these factors are expected to converge as more strong motion data becomes available.

In addition, the amplification factors (*AF*s) obtained for KDRA for short periods (T < 0.2 s) are greater than the unit (*AF* > 1). There is, however, a noticeable decrease in amplification for all periods beyond 0.2 s, resulting in *AF*s of approximately 0.6. This deamplification effect can be attributed to the presence of a geological formation, close to the surface, characterised by a high shear wave velocity (hard rock, V_s > 800 m/s).

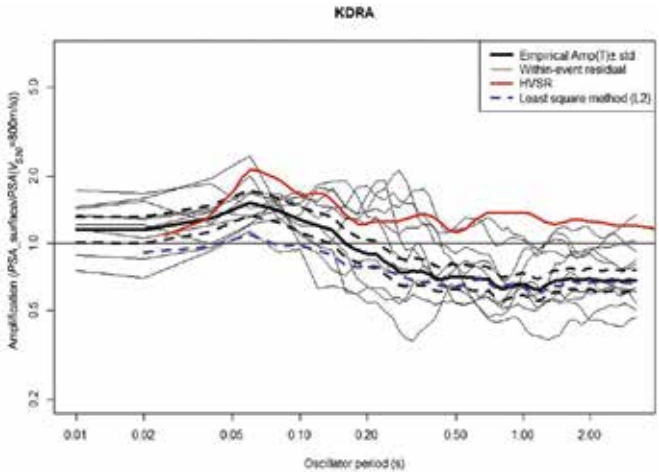

Fig. 8 - The empirical amplification functions for KDRA using both the MEA and L2 method.

Additionally, empirical amplification functions were obtained for several sites (Fig. 9). It is important to note that these sites have a smaller amount of data, which necessitates the exclusive use of the MEA.

Thus, the CRD station, significantly impacted by the 2003 Boumerdes earthquake, is considered as a firm site (S2) with V_{s30} around 480 m/s. Although the main shock was not recorded by this station, records of several aftershocks are available. Fig. 9 illustrates the within-event terms obtained for eight events ($M \geq 4.0$), with the derived site term (indicated with a solid black line) indicating an *AF* of approximately 1.3 for $T < 1$ s periods.

The TBL site in Tablet city, situated in a mountainous region, exhibits noteworthy amplification ($AF > 1.5$) during short periods ($T < 0.5$ s) based on the analysis of five events. Furthermore, there is a good agreement with the microtremor HVSR curve in terms of spectral ratio.

The EDB site is in Dar El Beida city, situated in the eastern part of Algiers, within the Mitidja basin. The site has a shear wave velocity (V_{s30}) of 500 m/s. Fig. 9 depicts the within-event terms obtained from the analyses of eight recorded earthquakes. Amplification function AF(T) is compared to the HVSR curve showing a good agreement in terms of fundamental period (T = 0.2 to 0.3 s). For long periods ($T > 1$ s), both the empirical results and the HVSR curve indicate amplification (*AF* approximately 1.2) of ground motion at the EDB site. However, amplification amplitudes are very different between the HVSR and empirical AF(T).

The BFK site, located in Boufarik city in the middle of the Mitidja basin, exhibits a different behaviour. It shows deamplification of ground motion during short periods ($T < 0.3$ s), whereas a clear amplification is observed for long periods ($T > 1$ s), in good agreement with the HVSR curve. This emphasises the basin effect at this site, where the geological features of the basin play a significant role in modifying the seismic response.

Considering the lack of in-depth studies on the basin effect in this region, and based on the empirical results obtained in this study, the use of an *AF* of approximately 1.6 for the BFK site in Boufarik, for periods longer than 1 s, is suggested. This *AF* is particularly relevant for long and flexible structures, such as high-rise buildings, which may be more susceptible to amplified ground motion in these areas.

The KTA and CGS sites are situated on the basin western edge. The KTA site has a shear wave velocity (V_{s30}) of 483 m/s, while the CGS site, near the CGS research centre, has a V_{s30} of 600 m/s. Results obtained for the CGS site indicate deamplification during short periods and significant amplification during long periods (Fig. 9). Similarly, the KTA station also exhibits amplification in

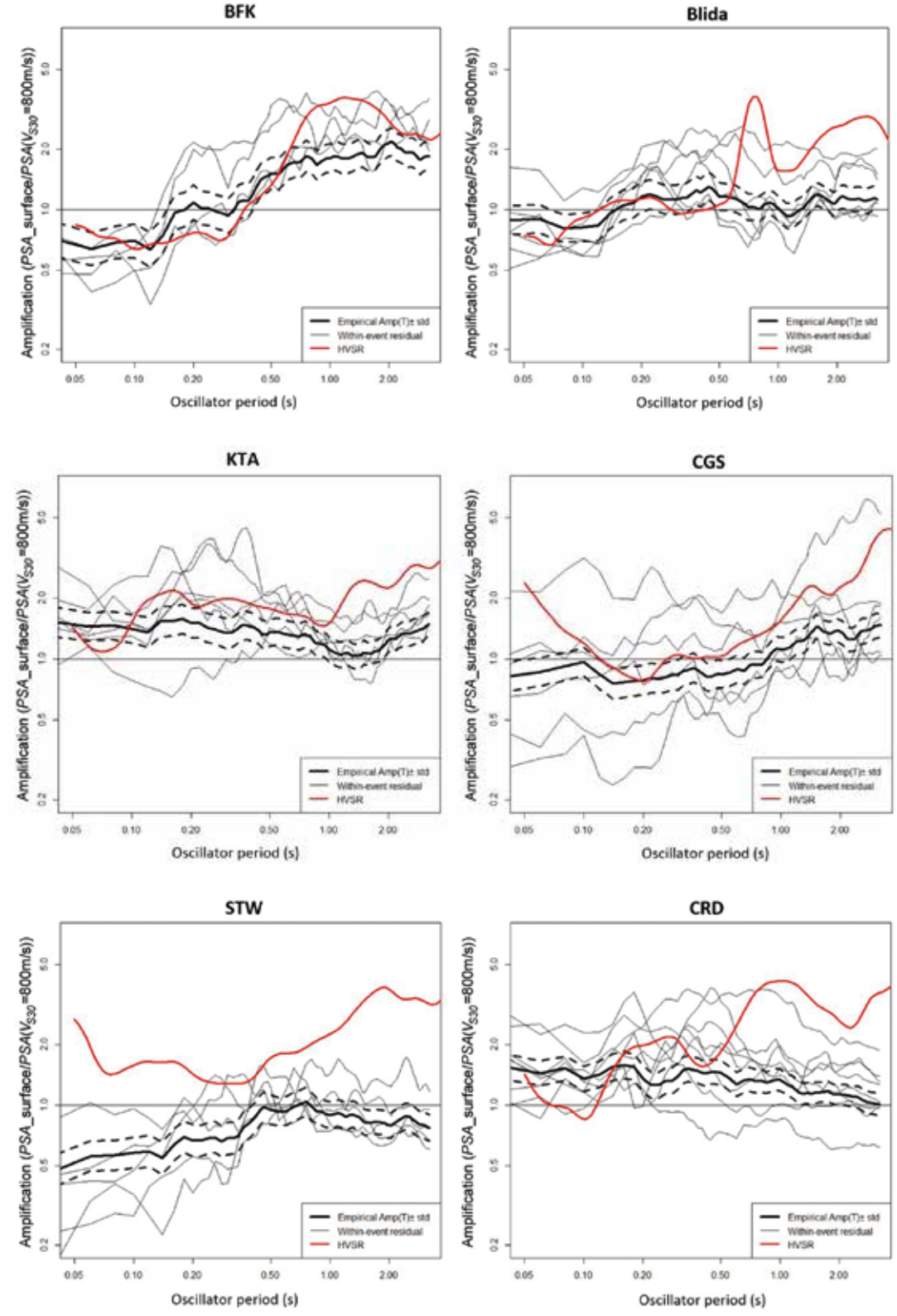

Fig. 9 - The empirical AFs(*T*) for selected sites (EDB, BFK, CGS, KTA, STW, BOZR, Blida and TBL stations).

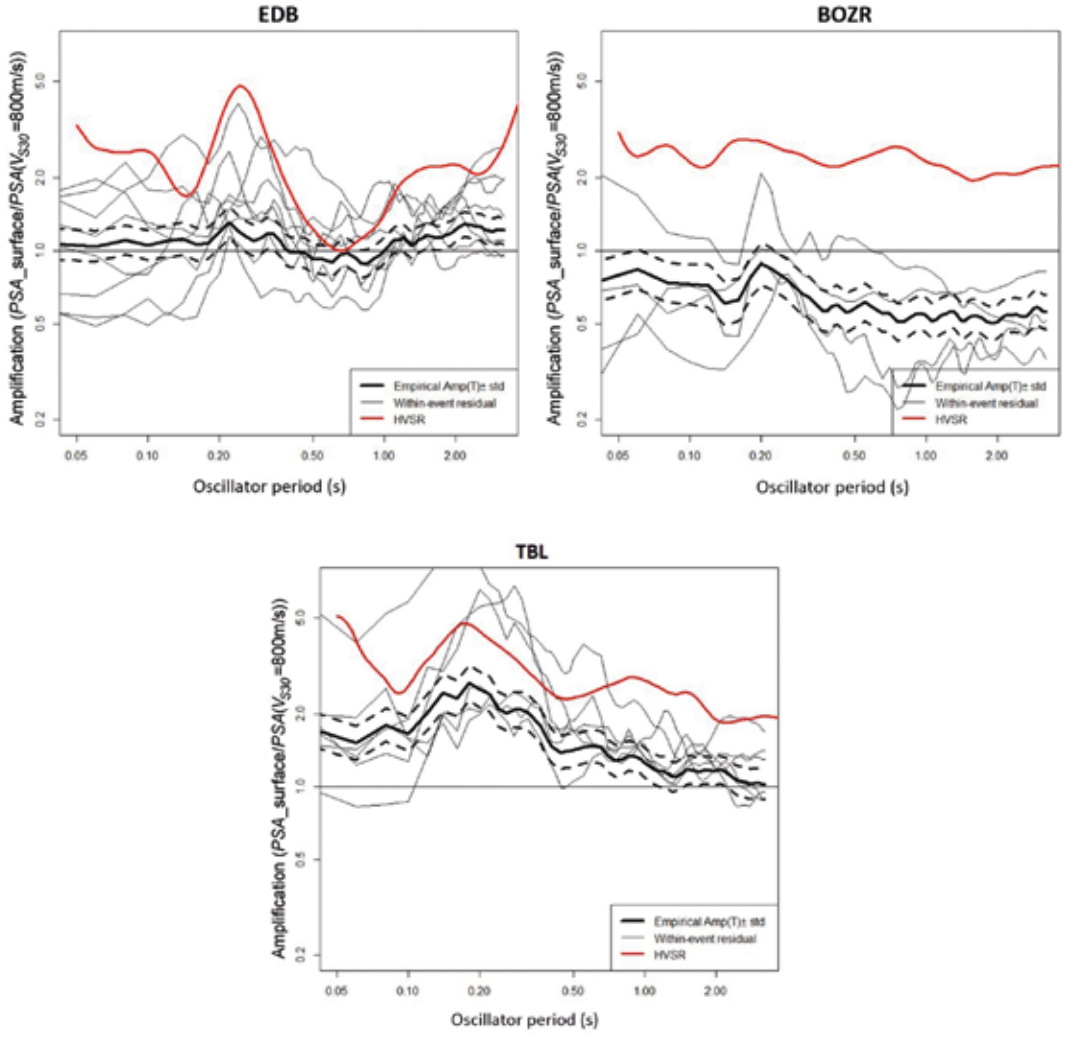

Fig. 9 - continued.

the long period range (Fig. 9). The empirical amplification functions obtained for both sites show a good agreement with the HVSR curve. However, further studies are necessary to investigate wave scattering and the generation of surface waves along the basin edge involving a numerical model of the 2D and 3D basin effect. The empirical AFs(*T*) obtained for the STW and BOZR sites, located on a rigid soil formation in Algiers city, as reported by JICA (2006), clearly prove this effect.

6. GMPE adjustment

In this section, empirical AFs(*T*), obtained in this study, are used to adjust the local GMPE with respect to the site effect by adding site term AF(*T*) to the general equation (Eq. 1), using the c_1 coefficient of the rock site (S1) [c_1 = 1.024 (V_{s30} ≥ 800 m/s)] as follows:

$$log_{10}PSA(T)^{surface} = log_{10}PSA(T)^{rock} + log_{10}\left(AF(T)\right) + \sigma(T). \quad (12)$$

Fig. 10 presents a comparison between recorded ground motions and surface predicted motions for the KDRA station, corresponding to several events recorded at the KDRA station.

The use of the adjusted GMPE significantly improves the prediction of ground motion compared to the observed motion for both short and long periods.

Fig. 11 displays the results for the BFK station. The use of the adjusted GMPE greatly enhances the accuracy of the prediction equation of this study in relation to the recorded motion mainly for long periods.

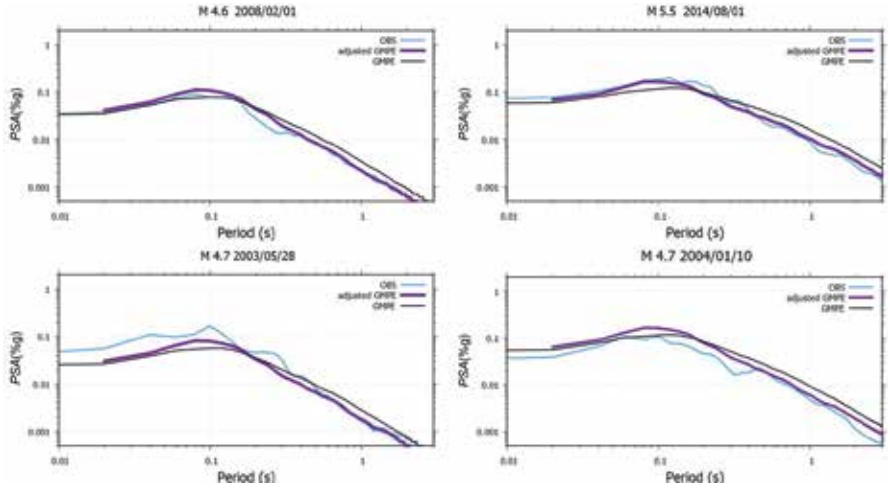

Fig. 10 - Comparison between the observed (OBS) and predicted (adjusted GMPE) surface ground motion for the KDRA site.

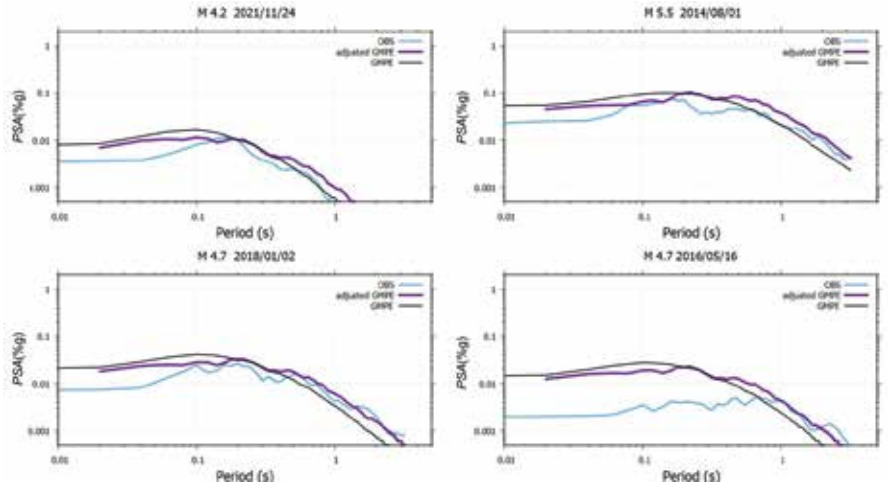

Fig. 11 - Comparison between the observed (OBS) and predicted (adjusted GMPE) surface ground motion for the BFK site.

Worthy of mention is the fact that, in addition to the site effect term, the between-event term is, at times, an important component in explaining the total residual between the predicted and the observed seismic ground motion.

7. Conclusions

Empirical AFs(*T*) have been developed for several sites in the central part of Algeria using strong motion data from a total of 17 earthquakes, ranging from magnitude M_W 4 to 6.8. Each earthquake event was recorded by at least three stations. The results are presented only for sites with a sufficient number of recorded events obtained by conducting the mixed-effects analysis on the total residuals of recorded ground motions relative to the local GMPE.

The first investigated site is KDRA, which is located on a rocky geological formation near the Keddara dam. For short periods, a slight amplification effect is observed when compared to the rock condition (V_{s30} = 800 m/s). However, for periods exceeding 0.2 s, a deamplification effect is observed with an *AF* of approximately 0.6. These findings are consistent with the results obtained from microtremor HVSR analyses, especially in terms of fundamental frequency and overall curve trend. Conversely, certain sites within the Mitidja basin, such as the EDB and BFK stations, clearly exhibit amplification effects at longer periods (T > 1.0 s). Expanding the data set can significantly enhance the accuracy of the estimated AFs(*T*) for each selected site.

Furthermore, an example of GMPE adjustment with respect to site effect is shown. The purpose of such adjustment is to enhance the accuracy of the surface ground motion predictions by incorporating empirical AFs(*T*). Hence, it is advisable to undertake partially non-ergodic approach for site-specific PSHAs in future research in Algeria.

REFERENCES

Abrahamson N.A. and Youngs R.R.; 1992: *A stable algorithm for regression analyses using the random effects model*. Bull. Seismol. Soc. Am., 82, 505–510.

Akkar S., Sandıkkaya M.A. and Bommer J.J.; 2014: *Empirical ground-motion models for point- and extended-source crustal earthquake scenarios in Europe and the Middle East*. Bull. Earthq. Eng., 12, 359–387, doi: 10.1007/s10518-013-9461-4.

Anderson J.G. and Brune J.N.; 1999: *Probabilistic seismic hazard analysis without the ergodic assumption*. Seismol. Res. Lett., 70, 19-28.

Atkinson G.M.; 2006: *Single-station sigma*. Bull. Seismol. Soc. Am., 96, 446-455.

Atkinson G.M.; 2015: *Ground motion prediction equation for small to moderate events at short hypocentral distances, with application to induced seismicity hazards*. Bull. Seismol. Soc. Am., 105, 981-992, doi: 10.1785/0120140142.

Baltay A.S., Hanks T.C. and Abrahamson N.A.; 2017: *Uncertainty, variability, and earthquake physics in ground motion prediction equations*. Bull. Seismol. Soc. Am., 107, 1754-1772.

Bates D., Maechler M., Bolker B. and Walker S.; 2015: *Fitting linear mixed-effects models using lme4*. J. Stat. Software, 67, 1–48.

Bensalem R., Chatelain J.-L., Machane D., Oubaiche E.H., Hellel M. and Guillier B., Djeddi M. and Djadia L.; 2010: *Ambient vibration techniques applied to explain heavy damages caused in Corso (Algeria) by the 2003 Boumerdes earthquake: understanding seismic amplification due to gentle slopes*. Seismol. Res. Lett., 81, 928-940, doi: 10.1785/gssrl.81.6.928.

Bensalem R., Chatelain J.-L., Machane D., Oubaiche E.H., Bouchelouh A., Benkaci N., Moulouel H., Chabane S. and Hellel M.; 2017: *Mediterranean Sea and anthropogenic influences on ambient vibration amplitudes in the low-frequency and high-frequency domains in the Algiers region*. Arabian J. Geosci., 10, 282, 12 pp., doi: 10.1007/s12517-017-3065-2.

Boore D.M., Stewart J.P., Seyhan E. and Atkinson G.M.; 2014: *NGA-West2 equations for predicting PGA, PGV, and 5%-damped PSA for shallow crustal earthquakes*. Earth Spectra, 30, 1057-1085.

Borcherdt R.D. and Gibbs J.F.; 1970: *Effect of local geological conditions in the San Francisco Bay region on ground motions and the intensities of the 1906 earthquake*. Bull. Seismol. Soc. Am., 66, 467-500.

Borcherdt R.D. and Glassmoyer G.; 1994: *Influences of local geology on strong and weak ground motions recorded in the San Francisco Bay region and their implications for site-specific building-code provisions.* In: Borcherdt R.D. (ed), The Loma Prieta, California, Earthquake of October 17, 1989 - Strong Ground Motion, U.S. Geological Survey, Denver, CO, USA, Professional Paper 1551-A, pp. A77-A108.

Guillier B., Chatelain J.-L., Hellel M., Machane D., Mezouer N., Bensalem R. and Oubaiche E.H.; 2005: *Smooth bumps in H/V curves over a broad area from single-station ambient noise recordings are meaningful and reveal the importance of Q in array processing: the Boumerdès (Algeria) case*. Geophys. Res. Lett., 32, L24306, 4 pp., doi: 10.1029/2005GL023726.

Hellel M., Chatelain J.L., Guillier B., Machane D., Bensalem R., Oubaiche E.H. and Haddoum H.; 2010: *Heavier damages without site effects and site effects with lighter damages: Boumerdes City (Algeria) after the May 2003 earthquake*. Seismol. Res. Lett., 8, 37-43, doi: 10.1785/gssrl.81.1.37.

Ibrahim R., Si H., Koketsu K. and Miyake H.; 2014: *Empirical spectral acceleration amplification in the Iwate-Miyagi and Niigata regions, Japan, inferred by a spectral ratio method using ground motion prediction equations*. Bull. Seismol. Soc. Am., 104, 1410-1429, doi: 10.1785/0120130124.

Japan International Cooperation Agency (JICA); 2006: *A study of seismic microzoning of the Wilaya of Algiers in the People's Democratic Republic of Algeria.* Nippon Koei Co. Ltd., Tokyo, Japan, Final Report, Vol. II, Main Report, 580 pp., < openjicareport.jica.go.jp/553/553_401.html >.

Laouami N. and Slimani A.; 2013: *Earthquake induced site effect in the Algiers-Boumerdes region: relation between spectral ratios higher peaks and observed damage during the May 21st Mw 6.8 Boumerdes*. Pure Appl. Geophys., 170, 1785-1801, doi: 10.1007/s00024-012-0612-3.

Laouami N., Slimani A. and Larbes S.; 2018: *Ground motion prediction equations for Algeria and surrounding region using site classification based H/V spectral ratio*. Bull. Earthquake Eng., 16, 2653-2684.

Parker G.A., Baltay A.S., Rekoske J. and Thompson E.M.; 2020: *Repeatable source, path, and site effects from the 2019 M 7.1 Ridgecrest earthquake sequence*. Bull. Seismol. Soc. Am., 110, 1530-1548, doi: 10.1785/0120200008.

R Core Team.; 2019: *R: a language and environment for statistical computing.* R Foundation for Statistical Computing, Vienna, Austria, < https://www.R-project.org/>.

Rodriguez-Marek A., Rathje E.M., Bommer J.J., Scherbaum F. and Stafford P.J.; 2014: *Application of single-station sigma and site response characterization in a probabilistic seismic hazard analysis for a new nuclear site*. Bull. Seismol. Soc. Am., 104, 1601-1619.

Sahakian V.J., Baltay A., Hanks T.C., Buehler J., Vernon F.L., Kilb D. and Abrahamson N.A.; 2019: *Ground motion residuals, path effects, and crustal properties: a pilot study in southern California*. J. Geophys. Res., 124, 5738–5753.

SESAME European Research Project (SESAME); 2004: *Guidelines for the implementation of the H/V spectral ratio technique on ambient vibrations measurements, processing and interpretation*. Bard P.-Y. (Coordinator), Project n. EVG1-CT-2000-00026 SESAME, European Commission - Research General Directorate, Bruxelles, Belgium, 62 pp.

Si H., Tsutsumi H. and Midorikawa S.; 2010: *Evaluation of hanging wall effects on ground motion attenuation relationship correcting the site effects*. In: Proc. 9th U.S. National and 10th Canadian Conference on Earthquake Engineering, Toronto, ON, Canada, Paper n. 467, 10 pp.

Stafford P.J.; 2014: *Crossed and nested mixed effects approaches for enhanced model development and removal of the ergodic assumption in empirical ground-motion models*. Bull. Seismol. Soc. Am., 104, 702-719.

Stewart J.P., Liu A.H. and Choi Y.; 2003: *Amplification factors for spectral acceleration in tectonically active regions*. Bull. Seismol. Soc. Am., 93, 332-352.

Stewart J.P., Afshari K. and Hashash Y.M.A.; 2014: *Guidelines for performing hazard-consistent one-dimensional ground response analysis for ground motion prediction*. PEER Report 2014/16, Pacific Earthquake Engineering Research Center, University of California, Berkeley, CA, USA, 139 pp.

Stewart J.P., Afshari K. and Goulet C.A.; 2017: *Non-ergodic site response in seismic hazard analysis*. Earthquake Spectra., 33, 1385-1414.

Wathelet M., Chatelain J.-L., Cornou C., Di Giulio G., Guillier B., Ohrnberger M. and Savvaidis A.; 2020: *Geopsy: a user friendly open source tool set for ambient vibration processing*. Seismol. Res. Lett., 1878-1889, doi: 10.1785/0220190360.

Zhao J.X., Irikura K., Zhang J., Fukushima Y., Somerville P.G., Asano A., Ohno Y., Oouchi T., Takahashi T. and Ogawa H.; 2006: *An empirical site classification method for strong strong-motion stations in Japan using H/V response spectral ratio*. Bull. Seismol. Soc. Am., 96, 914-925, doi: 10.1785/0120050124.

Corresponding author: Faouzi Gherboudj
National Center of Applied Research of Earthquake Engineering (CGS)
Rue Kaddour Rahim prolongé, H-Dey, Algiers 16000, Algeria
Phone: +213 (0) 555 448295; e-mail: fgherboudj@cgs-dz.org; gherboudj_faouzi@yahoo.fr